OXFORD INSTITUTE FOR RADIATION ONCOLOGY

MSc Radiation Biology

2019

Cycling Hypoxia and Radiosensitivity

Candidate No: 1031258

Word Count: 9,158

TABLE OF CONTENTS

ABSTRACT

While chronic and acute hypoxia are well-studied components of radiobiology, research is emerging that consistently describes transient and cyclic patterns of hypoxia within the tumour microenvironment. The aim of this study is to better understand the effect that cyclic hypoxia could have on radiotherapy. Using the breast cancer cell line, MDA-MB-231, and cycling between ≤0.1 O_2 and 2% O_2, I investigated the biological response to cyclic versus chronic hypoxia. The impact of cyclic hypoxia on cell cycle, DNA damage and the expression of homologous recombination protein, Rad51, were investigated. Cyclic hypoxia was found to cause a significant reduction in clonogenic survival. Most importantly, cells exposed to cyclic hypoxia were found to be more radioresistant that cells irradiated after exposure to constant hypoxia (2% O_2), but were not as radioresistant as cells exposed to near anoxic levels (<0.1% O_2).

1. INTRODUCTION

1.1 HYPOXIA AND CANCER

Since the first description of tumour vasculature being irregular in the mid 1800's, hypoxia has been implicated in the development of cancer (Virchow, 1863). The chaotic and rapid growth of solid tumours leads to poorly vascularised and hypoxic regions. At the cellular level, hypoxia occurs when oxygen concentrations are insufficient to meet metabolic demands (Wigerup, et al., 2016). An exact oxygen concentration for hypoxia cannot be defined as metabolic demands vary widely between tissue types. Physiologically 'normal' partial pressure of oxygen (pO_2) levels vary widely, from 4.6% in the brain, 5% in the liver, and 5.6% in the lung (Dings, et al., 1998) (Hammond, et al., 2014) (Koh & Powis, 2012) (Le, et al., 2006). As the maximum diffusion of oxygen in tissue has been measured to be approximately 150 μm, the ability for oxygen to reach tissue is primarily determined by the distribution of the tumour vasculature (Vaupel, 2004). Rapid proliferation in solid tumours results in a mass of tissue that is only peripherally supported by the surrounding stroma. This often leads to a well-perfused outer shell of tissue. However, this well supported shell leaves a hypoxic and often necrotic core at the centre of solid tumours as first described by Thomlinson & Gray (1955). As a tumour proliferates, multiple hypoxic cores can form. The harsh, chronically hypoxic environment outside of the diffusion-limited margin drives positive selection for aggressive phenotypes (Evans, et al., 2004) (Chang, et al., 2011). Some studies would estimate that 50-60% of solid tumours exhibit hypoxic regions (Vaupel & Mayer, 2007). It has been shown in a number of tumour types that hypoxic tumours are the most aggressive and therefore have the worst prognosis (Brahimi-Horn, et al., 2007). This makes hypoxia relevant across a panel of solid tumour types and all therapies. Increased aggression decreases the chances of curative surgery, while chemotherapy requires vascular access to cells to be effective. Radiotherapy as well is greatly impacted by lack of oxygen. Therefore, in order to improve patient response across all therapies, it is vital that we understand the biological response to hypoxia.

1.2 Hypoxia and radiation response

Hypoxia has long been recognised as a source of resistance to both radiation and chemotherapy (Brown & Wilson, 2004). Cells in near anoxic conditions can require two to three times the dose of radiation to achieve the same amount of cell kill, this is know as the oxygen enhancement ratio (OER) (Gray, 1953). Irradiation of cells induces DNA damage in two ways. Direct damage occurs when particles directly interact with the DNA helix. Indirect damage, the primary mechanism by which irradiation induces DNA damage, is hydrolysis of water to form radicals that subsequently react with molecular oxygen. This then generates oxygen-based radicals that interact with DNA inflicting permanent damage. Therefore, presence of molecular oxygen at the time of irradiation is key in achieving maximum DNA damage. It has been estimated that two thirds of the DNA damage incurred by x-ray radiation are indirect (in which a photon does not directly interact with a DNA helix) and is mediated by free radicals (Hall & Giaccia, 2019). Molecular oxygen is able to "fix" this indirect damage interacting with hydroxyl radicals (Grimes & Partridge, 2015). This action is independent of cell type, though it can be altered with the type of radiation. High linear energy transfer (LET) radiation is better able to overcome this feature.

Importantly, the level of hypoxia can modulate radioresistance. An idealized representation is found in **figure 1.1**. At 0 mm Hg (0% O_2), radioresistance is at maximum potential as there is no molecular oxygen available to fix indirect damage. However, a slight increase in oxygen concentration up to 0.5% O_2 can double the sensitivity of radiated cells. This is not a linear function of oxygen concentration, and the sensitivity is maximized at about three times the level of damage incurred in a complete lack of oxygen. This is maximized at around 30 mm Hg (5% O_2).

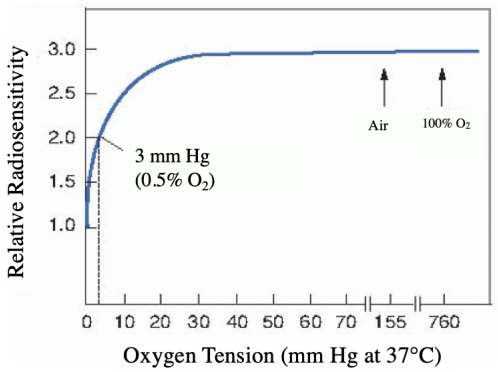

Figure 1.1 An idealized graph demonstrating the radiosensitizing properties of molecular oxygen. Radiosensitization increases dramatically with increase in oxygen concentration up until about 5% O_2, after which there is a plateau.

Maybe more importantly, this radioresistance has been correlated to patient prognosis in 1993 by using an electrode to measure O_2 concentrations (Höckel, et al., 1992). Patients with well-oxygenated tumours (defined as $pO_2 > 10$ mmHg) had nearly double the six-year survival probability of those with poorly oxygenated tumours with the same radiotherapy regimen. Hypoxia has since been recognised as the major resistance factor to radiotherapy.

1.3 Acute Hypoxia

Extensive research has been conducted on the effect of hypoxia on patient outcome, radiosensitivity, tumour progression, and drug interaction. Oftentimes, the hypoxic environment is modelled in laboratory setting by creating a near anoxic (≤0.1% O_2) level of O_2. While this is helpful in understanding chronically hypoxic regions of tumours—studies have shown that the tumour microenvironment is more intricate than a matter of diffusion limited oxygen levels. While highly vascularised, the periphery surrounding the chronically hypoxic core is plagued by arterial shunting, inefficient orientation, and slow blood flow (Dewhirst, 2009). Understanding the morphology and implications of this network lagged behind identifying the hypoxic core.

Using a sophisticated cell staining approach, Chaplin and Durand were able to show that cells in close proximity to blood vessels could still be highly radioresistant (Chaplin, et al., 1986). Hoechst 33342 (a DNA binding agent) was injected intravenously, quickly followed by irradiation and subsequent removal of the tumours. Tumours were then disaggregated into single cells and sorted by

flow cytometry based on Hoechst 33342 intensity. The higher a cell's intensity—the better access to a vessel it had and therefore better oxygenated it was reasoned. Successful uptake of Hoechst 33342 indirectly suggests successful oxygen delivery as well. These cells were then subjected to clonogenic assays to determine their surviving fraction. This approach determined that when Hoechst 33342 was administered simultaneously with radiation cells with more intense dye were more radiosensitive. All cells receiving the dye DNA binding agent had access to vasculature and were therefore well oxygenated at the time of radiation. However, when cells were irradiated 20 minutes post-injection there was no difference in radiosensitivity between cell populations that were well stained or poorly stained. This suggested that cells which had access to an oxygen supply at the time of injection (brightly dyed cells) had a significantly altered access by the time cells were irradiated. This was the realisation of acute hypoxia in the tumour environment and its drastic implications on radiotherapy.

Acutely hypoxic regions arise as a consequence of the temporary disruption to oxygen availability due to: static blood flow (a product of chaotic blood supply-shunting, interstitial pressure, and inefficient orientation); or due to a lapse in red blood cell (RBC) flux. When quantified, Bennewith et al. suggested 20% of a tumour could experience these rapid changes in oxygenation (2004). This chaotic model of chronic hypoxia in combination with acutely hypoxic portions complicates studying the response to radiotherapy. A chronically hypoxic cell's biology is greatly different (replicative stress, the HIF response) to that of a cell that has only been hypoxic for several minutes—though both are highly radioresistant. In fact, it is suggested that these acutely hypoxic cells are more radioresistant than their chronic counterparts due to their still being nutrient rich and able to undertake repair processes more successfully (Denekamp, 1999). Numerous studies have continued to support the finding of temporary loss in oxygen delivery, creating a picture of two basic types of hypoxia—Chronic and acute.

1.4 Cyclic Hypoxia

As our understanding of hypoxia has advanced alongside cancer therapeutics a two-category approach to hypoxia has been realised as an oversimplification. Using various means of detection (for example: paramagnetic resonance, labelled nitroimidazoles, and miRNA levels), acutely hypoxic regions have been found to have highly transient patterns. Rather than a temporary complete disruption to blood supply and therefore oxygen supply, many cells actual experience fluctuations (**figure 1.2**) (Horsman, et al., 2012). This adds another layer of untested complexity to the common laboratory model of studying hypoxia at constant levels.

From this model of fluctuating hypoxia, a pattern of cyclic oxygenation has been repeatedly recorded via several experimental methods. Using optical coherence tomography (OCT), Skala et al. observed patterns of cyclic oxygenation on the scale of several hours correlating with changes in vessel diameter, haemoglobin saturation, and blood velocity (Skala, et al., 2009). With red blood cell labelling and oxygen sensing electrodes, several studies have found that pO_2 levels are inversely related to

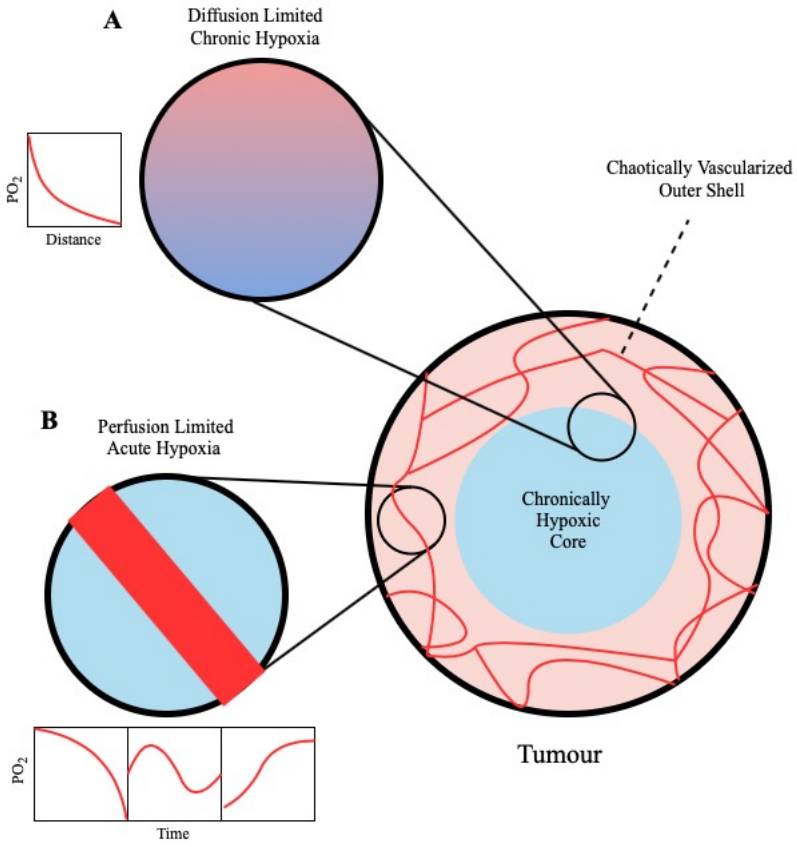

Figure 1.1 A The classic model of diffusion limited chronic hypoxia in which oxygenation is solely a function of vasculature layout. The generally well oxygenated shell fades into a chronically hypoxic core. **B** The model of transient acute hypoxia. Despite being located in a well vascularized portion of the tumour, oxygen delivery can be temporarily occluded. Fluctuations in oxygen can cover a large spectrum of patterns, including cyclical.

distance from microvessels and cyclic fluctuations occur independent of vascular stasis (Kimura, et al., 1996) (Lanzen, et al., 2006). These independent findings all show a pattern of oxygen fluctuations in cells. However, these studies often require window chambers or flow cytometry as an indirect means of inferring hypoxic status. Such invasive means or indirect means of determining oxygen fluctuations doesn't necessarily represent a what is occurring in vivo.

More convincingly, modern imaging techniques are able to visualise regions in a tumour subject to cyclical oxygen fluctuations directly. Baudelet et al. were the first to do this by utilising a T2* weighted CT scan, finding cyclic fluctuations in murine xenografts (Baudelet, et al., 2004). More recently, electron paramagnetic resonance imaging (EPRI) has been used by Yasui et al. to image fluctuations in murine tumours in 3D (**figure 1.3**) (2010). This method has several exciting advantages, which could all contribute to it one day being used clinically. It is non-invasive and does not employ a radioactive isotope, avoiding concern of unneeded radiation. In addition to these benefits, it is able to provide absolute pO_2 values with a resolution of 3-4 mmHg and 1-2 mm spatial resolution.

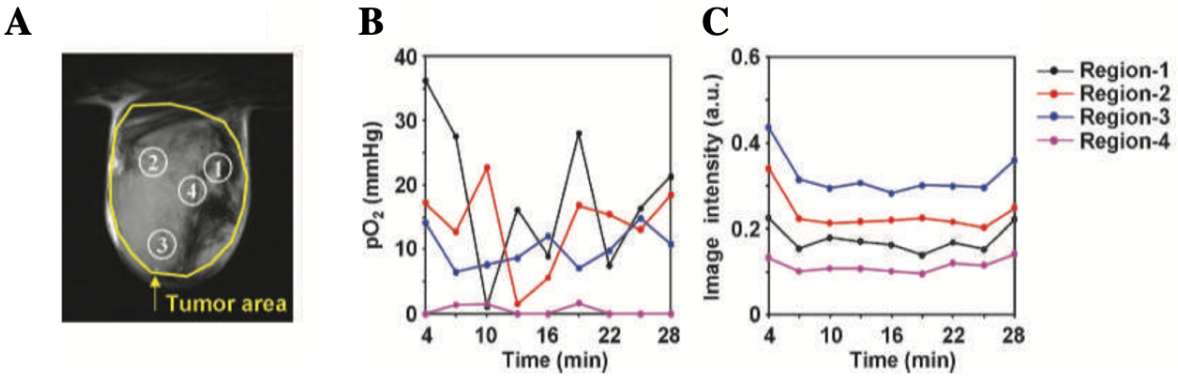

Figure 1.3 Evidence of cyclic hypoxia in murine xenografts utilising EPRI. A) A T_2 weighted image of the tumour being analysed for cyclic hypoxia. B) Levels of pO_2 within these regions can be seen to fluctuate. C) This measured difference in pO_2 is shown to be independent of any change image intensity. This reveals a highly heterogenous microenvironment with high variation. Importantly, spatially tangential regions 1 and 4 are greatly differentiated in fluctuations. This implicates that aspects of cyclic hypoxia (intensity in fluctuations and time scales) are highly varied within the tumour. Adapted from Baudet et al.

As a more detailed understanding of cyclic hypoxia emerges, the realisation that these dynamic processes are taking place in the clinic becomes unavoidable. This poses the question: how does cyclic hypoxia modify the tumour response to current therapeutics, in particularly radiotherapy? Again, whilst the cellular response to hypoxia at constant levels is a well-studied phenomenon, a detailed understanding of the radiotherapeutic response in cyclic hypoxia is poorly studied. As cancer therapy becomes progressively more personalised, the ability to match therapeutics to specific tumour phenotypes becomes a greater focus. As cyclic tendencies become possible to identify *in vivo* with imaging, identifying cyclic tumours could help guide treatment choices.

In summary, it appears a significant portion of tumours experience cyclical patterns of fluctuating hypoxia. A useful analogy to understand cyclic hypoxia has been proposed by Dewhirst (2009). Consider the tumour a Pacific island (**see figure 1.3**). Small islands at high tide may be completely covered by water, such that waves washing over it have no effect on how much of the beach is exposed. In the same way, cyclic waves of hypoxia are unlikely to have a great impact on chronically hypoxic tissue. However, at low tide, the island is now exposed, and the cyclic nature of waves greatly impact how much of the beach is covered at any given time. It is this "low tide" portion of the tumour that effected by cyclic hypoxia.

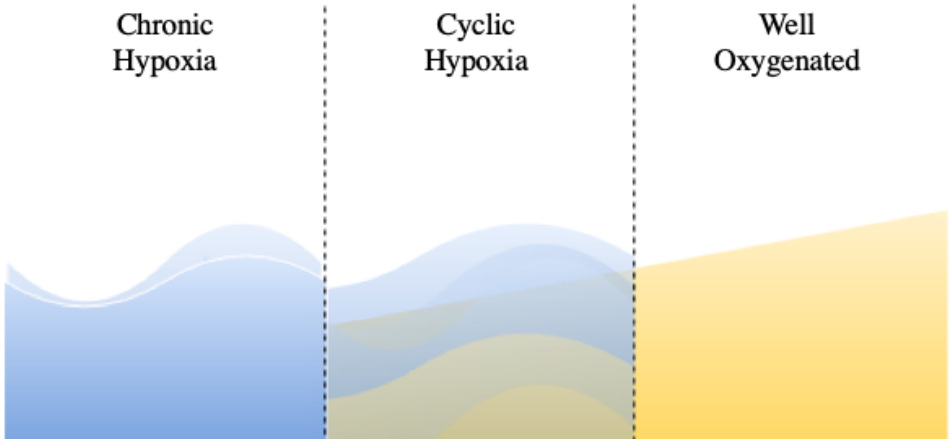

Figure 1.4 The analogy of tides and waves describing the impact of cyclic hypoxia on the tumour microenvironment. At regions of the beach where the tide completely covers the beach, waves make little impact on beach coverage. However, at low tide, the shore is cyclically covered in water by waves. In the same way, the effect of cyclic hypoxia is dependant on the region's groundstate of oxygenation.

1.5 Known Consequences of Cyclic Hypoxia

Some characteristics of tumours experiencing cyclic hypoxia have been studied. Cairns and Hill devised a system to induce cyclic hypoxia by switching mice from breathing atmospheric air to a gas mix with a relatively low oxygen concentration several times a day. In their cervical orthotopic model they found an increased rate of metastasis in regional lymph nodes (Cairns & Hill, 2004). Using this same model, an increase in the expression of genes associated with metastasis was found including CXR4, uPAR, and vascular endothelial growth factor (VEGF) (Chaundary & Hill, 2009). An increased metastatic phenotype is a reason why imaging of a patient's hypoxic profile is important; determining

if a tumour experiences cyclic hypoxia can indicate the potential for an aggressive phenotype, and possibly alter treatment strategy. This increased rate of metastasis could be a result of an enhancement of vasculature as better access to vasculature likely improves chances of intravasation. By using cycles of hypoxic gas to mimic cyclic hypoxia in mice, Rofstad et al. found amplified blood perfusion, increased microvascular density, and greater amounts of VEGF in melanoma xenografts (2010). With this increased vasculature, they also found an increase in pulmonary metastasis. Increased vascular availability is believed to offer enhanced availability to intravasation by cancer cells, a crucial step in the process of metastasis.

1.6 Reoxygenation Injury

A physiological concern of tissue cycling between hypoxia and a greater oxygen concentration is reoxygenation. The effects of reoxygenation are relatively well studied. The majority of medical knowledge on this topic results from the understanding of ischemia in myocardial infarction or stroke. Apoptosis is unlikely to occur under ischaemic (≤0.1% O_2) conditions, as it is an energy consuming process and the cell is unable to undertake metabolic processes. While apoptosis is a P53 driven response to low levels of oxygen, small populations of P53 mutated cells are often selected for in the tumour microenvironment and therefore become resistant to death as a result of chronic hypoxia (Graeber, et al., 1996). Cell death via apoptosis is also a cellular response due to reoxygenation (Saikumar, et al., 1998). In this way reoxygenation is both beneficial and harmful to tissue, which needs oxygen to metabolise, yet is damaged in the process of reoxygenation. This is due to production of reactive oxygen species (ROS) being produced during the reactivation of the electron transport chain. Casapase-9 and -3 are known to be responsible for subsequent triggering of the apoptotic cascade following these mechanisms (Ho, et al., 2006).

1.7 DNA Damage Response

A crucial feature that impacts response to radiotherapy is the DNA damage response (DDR). In constant hypoxia, it is well established that DNA repair is downregulated at a wide range of levels

of hypoxia (Bristow & Hill, 2008) (Bindra, et al., 2004). However, constant exposure to <0.1% O_2 activates ATR/ATM signalling (Hammond, et al., 2003). Despite this, there is no 53BP1 foci formation (Bencokova, et al., 2009). Additionally, the commonly used marker of damage, γH2AX, is phosphorylated in hypoxia but is pan-nuclear as opposed to forming discreet nuclear foci (Olcina, et al., 2014). It then seems that despite activation of the DNA damage response in hypoxia, there is no actual DNA damage in hypoxia.

Repeated reoxygenation injury, as might be experienced in cyclic hypoxia, could be expected to upregulate damage markers and repair machinery. It is also possible that if oxygen supply is disrupted often, the DDR would eventually become unable to cope with this injury. Understanding the DDR in cyclic hypoxia is an important predicter of the radiotherapy response.

1.8 Project Aims

The goal of this project is to determine the affect of cyclic hypoxia on factors that contribute to radiosensitivity, and ultimately whether cyclic hypoxia modifies the radiosensitivity of cells. As controls, results will be compared with the known effects of radiobiological hypoxia (0.1% O_2) and less severe hypoxia (2% O_2). Factors effecting radiosensitivity studied will include the cell cycle, DNA Damage, DDR, and finally clonogenic survival.

2. Materials and Methods

2.1 Tissue Culture

Unless otherwise stated, MDA-MB-231 cells [European Collection of Authenticated Cell Cultures] were used. All cells were cultured in Dulbecco's Modified Eagles Medium (high glucose) supplemented with 10% foetal bovine serum (FBS) in addition to 1% penicillin and streptomycin. Cells were grown in a humidified incubator at 37°C and 5% CO_2. Routine tissue culture involved removal of medium, washing with PBS, followed by a three-minute trypsinisation using Trypsin EDTA solution (Sigma). Trypsin was then inactivated using fresh media. This suspension was then centrifuged at 1500 rpm and the supernatant was removed. Cells were then resuspended in fresh media. Cell density was determined using a haemocytometer. The desired numbers of cells were seeded in fresh media prior to any experiments.

2.2 Hypoxic Conditions

2.2.1 Constant Hypoxia

For cells subjected to constant oxygen levels of less than 0.1% O_2, cells were treated in a Bactron II Anaerobic Chamber (Shell Labs). As oxygen is known to leach to plastics, solutions and plastics were equilibrated to ≤0.1% O_2 before use.

2.2.2 Cyclic Hypoxia

A Don Whitley (M35) Chamber was used to alternate between <0.1% and 2% O_2. The chamber was programmed to spend 105 minutes at each condition while taking 15 minutes to switch from the last setting for a total of 2 hours at each setting and 4 hours for each cycle. Unless otherwise stated, this cycle was used for all cyclic conditions.

2.3 Irradiation

Irradiations were carried out using a Gamma Service® GSR D1 irradiator which contains a Cs^{137} source. The dose rates were 1.938 Gy/min and 1.233 Gy/min (depending on the distance from the source) as determined by the manufacturer. Samples were placed at the appropriate position and

exposed to the required dose. The exposure time was calculated according to the dose rates of the system. In cases of clonogenic assay irradiation, airtight boxes were used to transport cells from both hypoxic chambers to maintain oxygen levels through irradiation.

2.4 Protein lysate preparation

Cells were seeded at 60-70% confluency and collected at oxygen levels described in each experiment. First, cells were decanted of media and washed with 1 mL of PBS. Then, they were scraped into 1 mL of PBS and spun down to remove the supernatant and resuspended in 90-120 µL of UTB buffer (9 M urea, 75 mM Tris HCl, pH 7.5, 0.1 M β-mercaptoethanol). Samples were sonicated for 2 cycles of 20 seconds on and 5 seconds off and then centrifuged at 16.2 x g for 10 minutes at 4°C. The supernatant was then transferred to a new container and 2 µL of this solution was used to determine protein density using a Nanodrop meter reading absorbance at 280 nm.

2.5 Western Blotting

Samples were normalised so that each sample contained 50 µg of protein and suspended in SDS buffer (1% SDS, 10mM EDTA, 50 mM Tris-HCl pH 8.1 and 25x complete Pi in Milli Q H_2O) then boiled at 100°C for 10 minutes. PROTEAN® TGX™ precast gels (BioRad) were used and 5 µL of a protein ladder was included on all gels (BioRad). Gels were electrophoresed at 100 V for 60 to 90 minutes in Tris-glycine running buffer (25 nM Tris base, 192 nM glycine, 0.1% SDS). Protein was then transferred onto a nitrocellulose membrane (BioRad). Membranes were then blocked using a LiCor Odyssey buffer diluted 1:2 in TBS for 1 hour. Membranes were probed with primary antibody (diluted in 1:1 LiCor Odyssey buffer:TBS-Tween) and incubated overnight at 4°C while shaking. Membranes were then washed with TBS-Tween three times and probed with either Alexa Fluor 680 or Alexa Fluor 800 (diluted 1:10,000) for 90 minutes. Membranes were then washed three times in TBS-Tween and subsequently scanned using an Odyssey infrared imaging system. Relative protein levels were quantified using ImageJ.

Table 2.1 Antibodies used in western blotting

Antibody Name	Species	Dilution	Supplier
H3	Mouse	1:1,000	Santa Cruz
H3 Ser10	Rabbit	1:1,000	Bethyl/Universal Biologicals Cambridge
p53	Mouse	1:2,000	Santa Cruz
p53 Ser15	Rabbit	1:1,000	Cell Signalling Technology
KAP1	Rabbit	1:1,000	Bethyl/Universal Biolgicals Cambridge
KAP1 Ser824	Rabbit	1:1,000	Bethyl/Universal Biologicals Cambridge
β-Actin	Mouse	1:10,000	Santa Cruz Biotechnology
H2AX	Rabbit	1:1,000	Calbiochem
γH2AX	Mouse	1:1,000	Millipore
RAD51	Rabbit	1:1,000	Cell Signaling Technology

2.6 Clonogenic Survival Assay

MDA-MB-231 Cells were seeded at a density of 700 cells per well of a 6 well plate for a period of 4 hours before being subjected to hypoxic conditions in order to allow cells to adhere. After being subjected to hypoxic conditions and in some cases irradiated, plates were returned to incubation conditions identical to standard cell culture for 7-9 days. Following this period, cells were stained with crystal violet dye (Sigma) for 30 minutes, washed, and dried. Colonies containing 50 or more cells were

defined as a single colony and counted. The plating efficiency and surviving fraction was calculated and tested for significance using a two-tailed, paired, univariate T-test.

2.7 Fluorescence Activated Cell Sorting

2.7.1 Bromodeoxyuridine/Propidium iodide

The thymidine analogue bromodeoxyuridine (BrDU) was used as an indicator of DNA synthesis in combination with propidium iodide (PI) staining to determine cell ploidy. Cells were harvested with 1 mL of trypsin and suspended in an additional 2 mL of Dulbecco's modified eagle's Medium high glucose (with 10% foetal bovine serum) while still at desired hypoxic levels of ≤0.1%, 2%, or 21% O_2. Samples where centrifuged at 252 g for 5 minutes, supernatant was removed, and cells resuspended in 1 mL of 70% ethanol in PBS for fixation in 21% O_2 conditions and frozen until processing. Samples were then centrifuged at 252 g for 5 minutes and ethanol was removed. Samples were denatured in 1 mL of 2 M HCl solution with a protease inhibitor (0.1 mg/mL Roche Diagnostics) and incubated at room temperature for twenty minutes. These were then centrifuged at 252 g for 5 minutes, ethanol removed, and resuspended in 2 mL of PBS. These were again centrifuged at 252 g for 5 minutes, supernatant removed, and resuspended in a PBS solution containing 2% foetal bovine serum. Primary BrDU antibodies (Becton Dickonson) were diluted 1:50 in PBS/2% foetal bovine serum solution. Samples were suspended in 100 µL of this solution overnight on a shaker at 4°C. Afterwards, 1 mL of PBS was added to samples and were subsequently centrifuged to remove the supernatant. Cells were then resuspended in 100 µL of a secondary fluorescent antibody (Alexa Fluor 488) that was diluted 1:200 in PBS/2% foetal bovine serum. This suspension was incubated for 60 minutes in the dark. To wash the cells, 1 mL of PBS was added to the suspension and again they were centrifuged to remove supernatant. Finally, the cells were resuspended in 1 mL of a propidium iodide (PI) solution made of PBS with 2% PI (Sigma Aldrich) and 0.5% RNaseA (Thermo Scientific). These were incubated for 30 minutes at 37°C. Cells were then fluorescently sorted using a BD FACSCalibur system.

2.7.2 Histone H3 ser10/Propidium Iodide

To use cells sorting to analyse mitosis, histone H3 ser10 was used as a marker of mitosis. After being subjected to aforementioned hypoxic conditions, cells were decanted of media, trypsinised in 1 mL of trypsin and then suspended in additional 2 mL of media while still in the chamber if applicable. These solutions were then centrifuged at 252 g for 5 minutes in normoxic conditions and supernatant was discarded. Cells were then suspended in 1 mL of 70% ethanol in PBS and frozen at -20°C for fixation. These solutions were then centrifuged at 447 g for 5 minutes and ethanol was removed. 1 ml of PBS was added to wash off excess ethanol and cells were again centrifuged at 447 g for 5 minutes to remove PBS. Cells were then suspended in PBS solution containing 2% FBS. Following this, these solutions were centrifuged at 447 g for 5 minutes, supernatant was removed, and cells were suspended in 100 μL of 1:200 phospho-histone H3 Ser10 antibody (Cell Signaling/New England Biolabs) in PBS/2% FBS and incubated on a shaker for an hour. After this period, 1 ml of PBS was added followed by centrifugation at 447 g for 5 minutes and decanting of resulting supernatant. Cells were then suspended in 100 μL of 1:200 Alexa Fluor 488 in PBS/2% FBS for one hour on a shaker in the dark. Finally, the cells were resuspended in 1 mL of a propidium iodide (PI) solution made of PBS with 2% PI (Sigma Aldrich) and 0.5% RNaseA (Thermo Scientific). These were incubated for 30 minutes at 37° C. Cells were then fluorescently sorted using a BD FACSCalibur system.

2.7.3 Cell Sorting Analysis

Doublet cell and live cell gating was processed using FlowJo (version 10). Analysis of cell cycle position using PI profiles and BrDU/PI plots were also done using Flowjo. Significance of these populations was accessed using a two-tailed, paired, univariate T-test.

2.8 Immunofluorescence Microscopy

To image 53BP1 foci, cells were seeded at 60-70% confluency in glass dishes over cover slips. After treatment in planned oxygen conditions, media was discarded, cells were washed in PBS, then fixed in 4% paraformaldehyde for 12 minutes. Paraformaldehyde was then washed off with PBS three times and kept in PBS at 4° C until processing. To permeabilise cells, a 1% triton in PBS solution was

used for 10 minutes. This was followed by a PBS wash and a one-hour incubation in a 2% BSA, 0.1% tween PBS solution for 1 hour. Each slide was then probed with 150 μL of 1:500 53BP1 antibody (Novus) in 2% BSA/0.1% tween PBS for 90 minutes. Slides were then each washed three times in cold 0.25% PBS tween and then incubated in 150 μL of 1:250 Alexa Fluor 488 in 2% BSA/0.1% PBS Tween for 90 minutes. Slides were again washed three times in 0.25% PBS Tween. Slides were then mounted in ProLong® Gold mounting Medium with DAPI (Invitrogen/Life Technologies). Slides were kept in the dark at 4° C before being analysed using a LSM780 (Carl Zeiss Microscopy Ltd) confocal microscope. Images were processed and cells determined to contain foci resembling that of the positive control were counted. Significance was tested using a using a two-tailed, paired, univariate T-test.

3. RESULTS

3.1 THE CELL CYCLE RESPONSE TO CYCLIC HYPOXIA DIFFERS TO CONSTANT HYPOXIA

To investigate the effect of cycling on the cell cycle, MDA-MB-231 cells were exposed to either normoxia (21% O_2), constant levels of hypoxia (≤0.1%, 2% O_2) or cyclic conditions (≤0.1-2% O_2) (shown schematically in **Figure 3.1**) and propidium iodide (PI) incorporation determined (**Figure 3.2**).

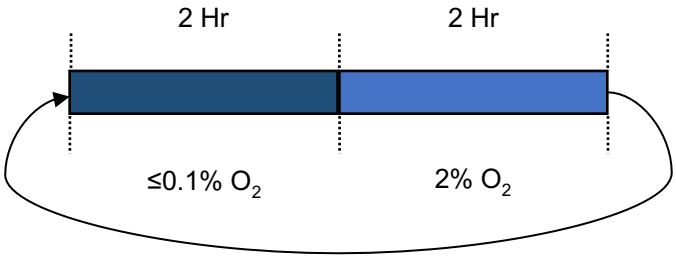

Figure 3. 1 Schematic representation of the cyclic hypoxia conditions used unless otherwise stated.

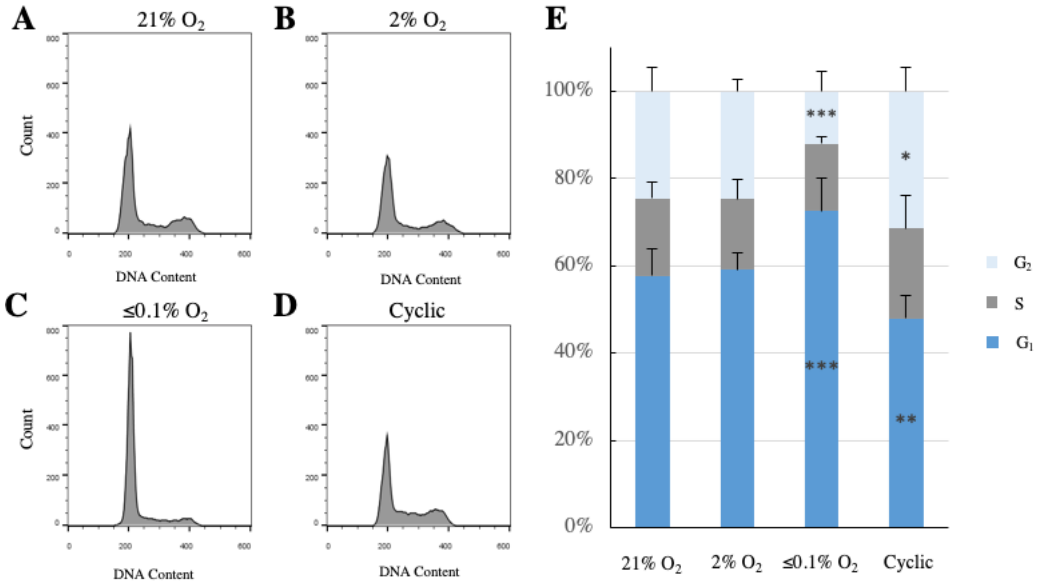

Figure 3.2 Cyclic hypoxia induces G_2 accumulation in MDA-321 cells **A-D**. MDA-321 cells were exposed to 21% O_2 (**A),** 2% O_2 (**B**), ≤0.1% O_2 (**C**), or cyclic hypoxia (**D**) for 20 hours. Cells were then fixed and stained with propidium iodide. Propidium iodide staining was measured using flow cytometry. **B**. Propidium iodide staining quantification shows a significant difference in G_1 and G_2 in ≤0.1% O_2 as well as cyclic conditions compared to normoxic conditions. n=3. Significance: * $P \leq 0.05$, ** $P \leq 0.01$, *** $P \leq 0.001$.

These data demonstrated that after exposure to 2% O_2, which is known to induce HIF-1alpha signalling and a hypoxic response, there was no significant difference in the cell cycle profile compared to the cells in normoxic conditions (**Figure 3.2A, B**). In contrast, exposure to ≤0.1% O_2 led to a significant accumulation in the G_1 phase of the cell cycle compared to normoxic (**Figure 3.2C**). The cell cycle in cyclic conditions did not include a G_1 accumulation as seen in response to ≤0.1% O_2 despite including periods of 2 hours at ≤0.1% O_2 (**Figure 3.2D**). Quantification of the numbers of cells in each phase in each condition demonstrated that the cell cycle response to cyclic hypoxia was distinct to both constant exposure to 2 and ≤0.1% O_2. Specifically, T-test analysis supported that cyclic conditions resulted in a greater proportion of cells than were in the G_2 phase compared to all other normoxic, 2% O_2 and ≤0.1% O_2 ($P=5.38x10^{-5}$, $3.16x10^{-2}$, and $7.22x10^{-6}$, respectively).

3.1.2 DNA REPLICATION IN CYCLIC VERSUS CONSTANT HYPOXIA

To further investigate the cell cycle response to hypoxia, and specifically DNA replication in S phase, I determined BrDU incorporation in each condition. This allowed me to capture information on whether cells were actually incorporating nucleotides or if replication had stalled between G_1 and G_2. MDA-MB-231 cells were labelled with BrDU in 21, 2, ≤0.1%, or cyclic oxygen levels. These cells were sorted using FACS and analysed (**Figure 3.3**).

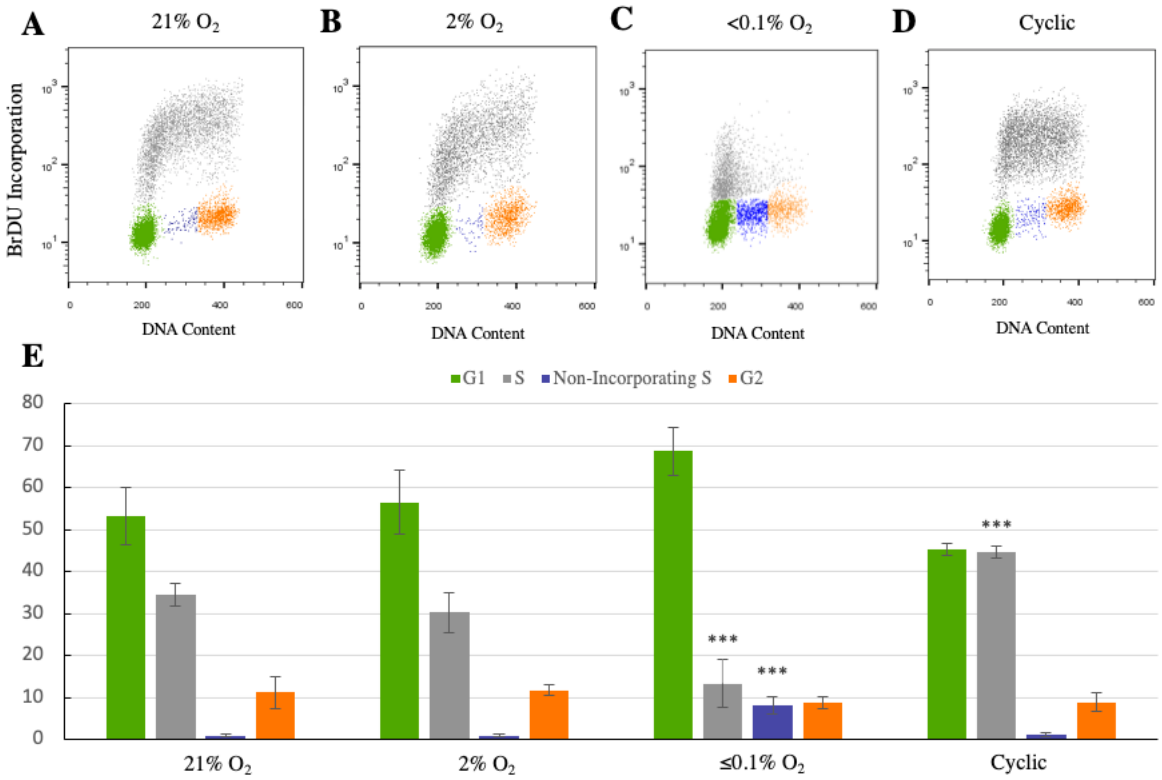

Figure 3.3 Cyclic hypoxia leads to an S phase accumulation. A-D**)** MDA231 cells were labelled with BrDU in the oxygen conditions indicated. Cells were then probed using a BrDU antibody and stained with PI. E**)** Quantification of percentage of cells in G1, S, Non-incorporating S, and G2 phase of the cell cycle. n=3. T-test comparing 21% O_2 to all other populations was used to analyse data. Significance: *** $P \leq 0.001$.

As expected, cells in normoxic gave the typical 'horseshoe' pattern (**Figure 3.3A**) indicating that the cells in S phase were actively incorporating BrDU and therefore synthesising DNA. Also, as expected, the cells in 2% O_2 appeared the same as those in normoxia i.e. this level of hypoxia had no impact on DNA replication (**Figure 3.3B**). As previously reported, exposure to ≤0.1% O_2 led to a complete loss of actively DNA synthesising S phase cells (**Figure 3.3C**) (Hammond, et al., 2004). Again, in contrast to either constant level of hypoxia, exposure to cyclic hypoxia gave a distinct response. In cyclic hypoxia the number of cells actively incorporating BrDU increased compared to all other conditions (**Figure 3.3D, E**). This S phase accumulation appears to create a reduction in the G1 population.

3.1.3 MITOSIS IN CYCLIC VERSUS CONSTANT HYPOXIA

Finally, I used the mitotic marker Histone 3 (H3) Serine (Ser) 10 phosphorylation to determine the impact of hypoxia (constant and cyclic) on mitosis. (**Figure 3.4**)

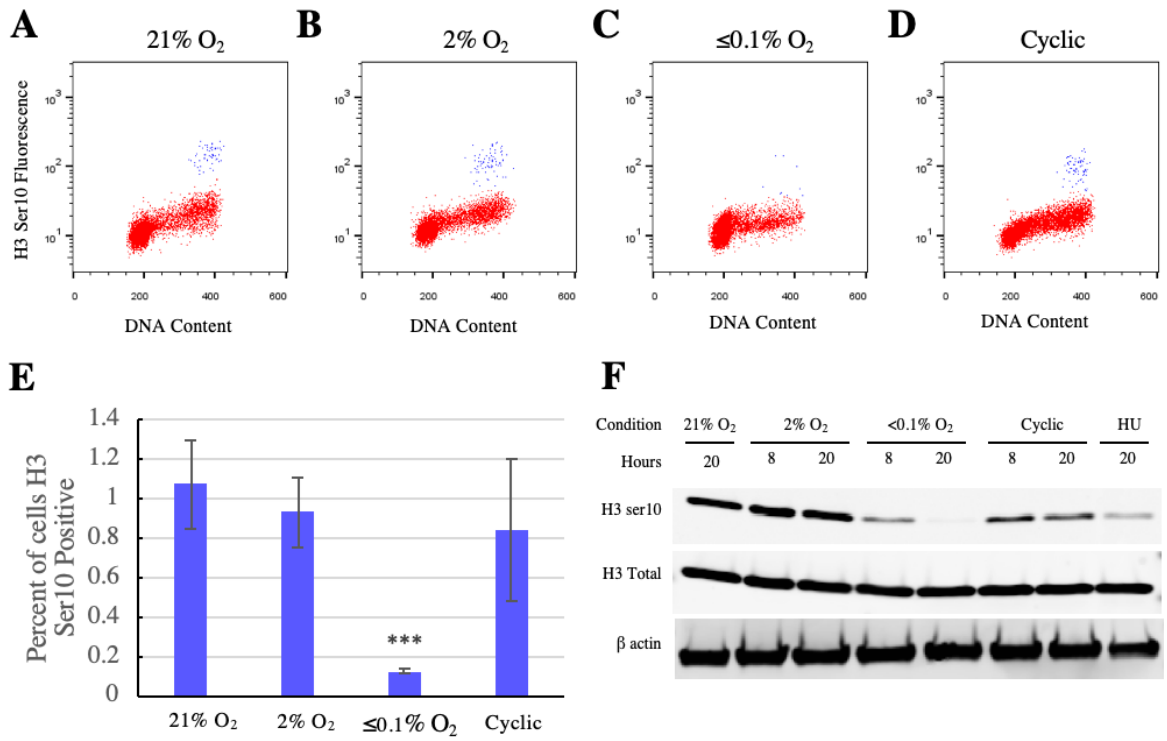

Figure 3.4 Cyclic hypoxia does not affect mitotic index. A-D) Characteristic FACS plots of H3 Ser10 intensity versus DNA content. E) Quantification of mitotic cells from these profiles using methods described in section 2.7.3 from n=3. F) Western blot demonstrating the disappearance of H3 ser10 with continued extreme hypoxia or when exposed to a damaging agent (HU) as is expected. Histone H3 continues to be phosphorylated in hypoxia (2% O_2) and in cyclic conditions. Significance: *** $P \leq 0.001$.

MDA-MB-231 cells were exposed to hypoxia followed by staining for H3-Ser10 and FACs analysis. No changes in the mitotic index were determined except for in the ≤0.1% O_2 conditions, which led to a significant decrease in the number of H3-Ser10 positive cells. To confirm this finding, I also carried out western blotting for H3-Ser10 in the same conditions (**Figure 3.4F**). These data again suggested that exposure to ≤0.1% O_2 had the most significant effect on H3-Ser10 levels although the cyclic conditions also seemed to lead to deceased expression. Overall these data suggest that cells in cyclic conditions continue to cycle as opposed to those in ≤0.1% O_2.

3.2 THE HYPOXIA-INDUCED DNA DAMAGE RESPONSE

Next, I investigated the (DDR) in each of the hypoxic conditions. For this analysis I used western blotting for the well-characterised DDR markers KAP1-S824 and γH2AX. KAP1 is phosphorylated by ATM and therefore a marker of damage and chronic hypoxia signalling.

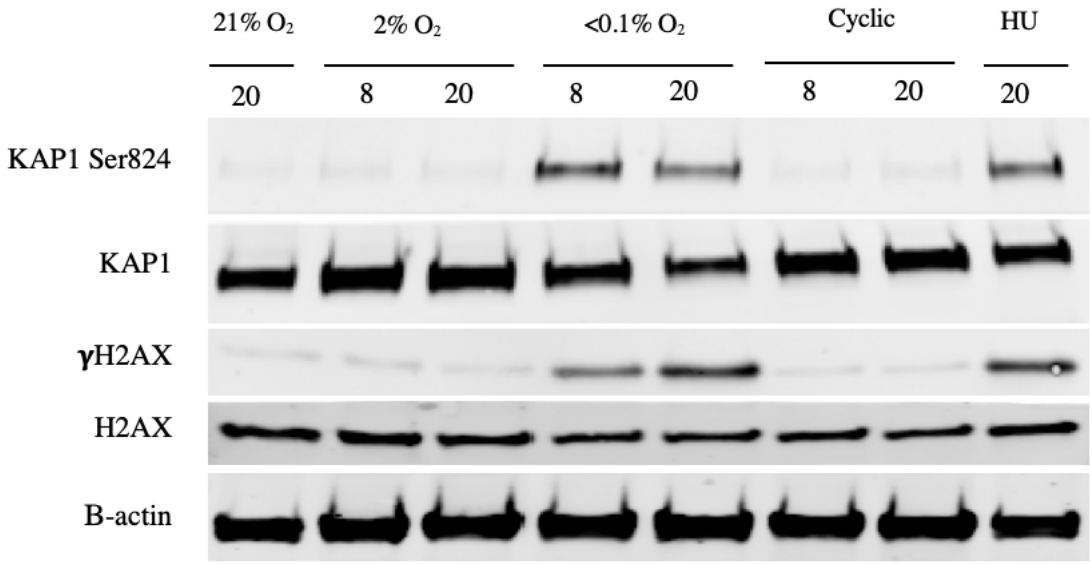

Figure 3.5 Cyclic hypoxia does not induce a DNA damage response. MDA-MB-231 cells were exposed to hypoxic conditions as labelled and lysates were probed with antibodies indicated. β -actin was used as a loading control while DNA damaging agent Hydroxyurea (HU) at 2 mM was used as a positive control.

As expected, ≤0.1% O_2 led to a rapid accumulation of both KAP1-S824 and γH2AX (Olcina et al., 2013). Neither the cyclic conditions of 2% O_2 resulted in any change in these DDR markers (**Figure 3.5**). To further determine if cyclic hypoxia could result in DNA damage, a 53BP1 foci assay was carried out. 53BP1 acts as a marker of DNA double strand breaks and promotes non-homologous end joining. MDA-MB-231 cells were exposed to cyclic hypoxia for a range of times followed by immunofluorescent staining for 53BP1. As a positive control cells were exposed to 4 Gy of radiation.

The cells in cyclic conditions were fixed as indicated in the schematic while the irradiated cells were fixed 1 hour after radiation (**Figure 3.6A**).

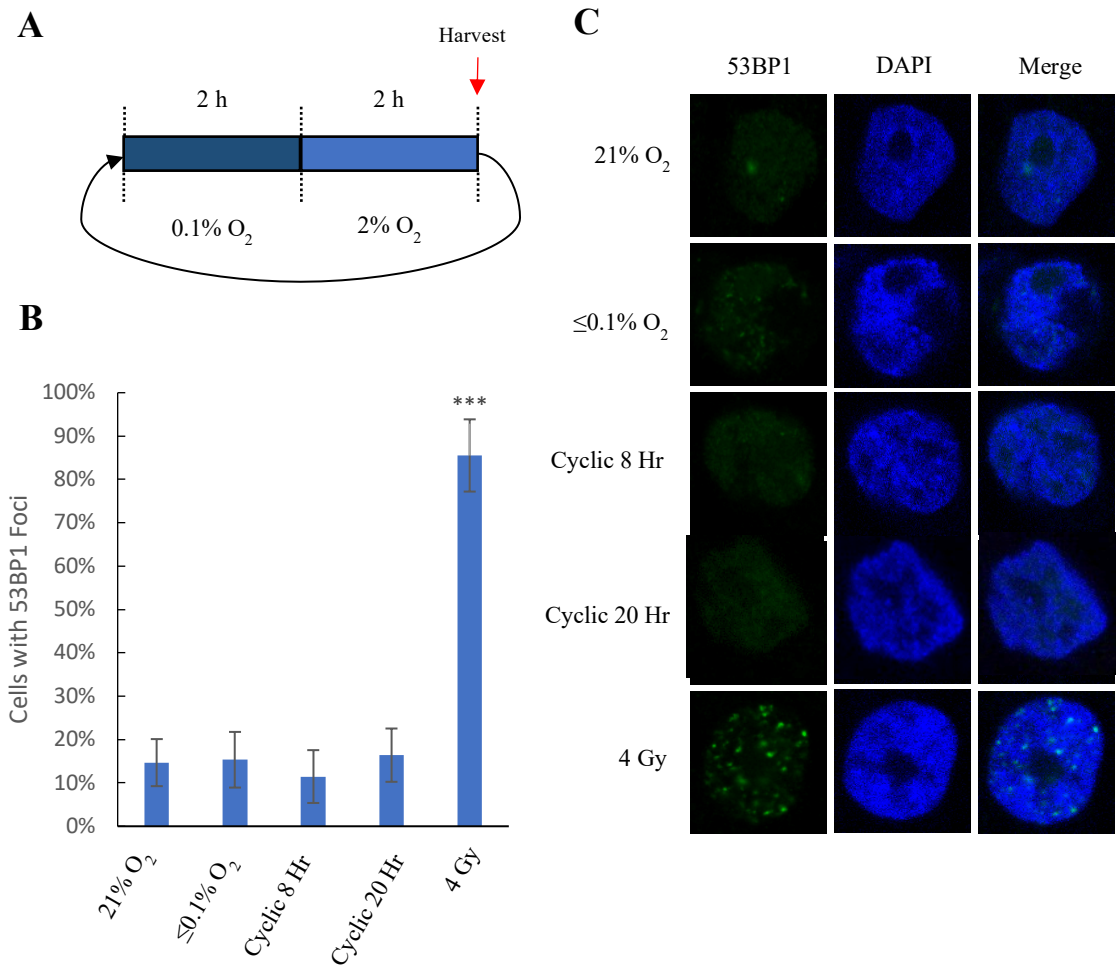

Figure 3.6 Cyclic hypoxia does not lead to DNA damage. A cyclic model of 2 hours at ≤0.1%O_2 and 2 hours at 2% O_2 does not lead to an accumulation of DNA damage. A) Diagram demonstrating when cells were fixed if harvested in cyclic conditions. B) Quantification of cells with 53BP1 foci from n=3. Significance: *** P ≤ 0.001. C) Representative images of cells probed for 53BP1 and stained with DAPI.

No increase in DNA damage was detected in cyclic cells (**Figure 3.6B**). This finding was somewhat surprising, as reoxygenation has been demonstrated to induce DNA damage previously. I hypothesised that the exact cycling conditions might determine the level of DNA damage and so I investigated alternative cycling parameters (**Figure 3.7A**). Knowing that reoxygenation should cause DNA damage, I shortened the period of oxygenation in order to reduce the length of time in which it

was possible for cells to undertake DNA repair. Preliminary data from these cyclic conditions suggested that DNA damage was indeed induced as determined by an increase in 53BP1 foci (**Figure 3.7B, C**).

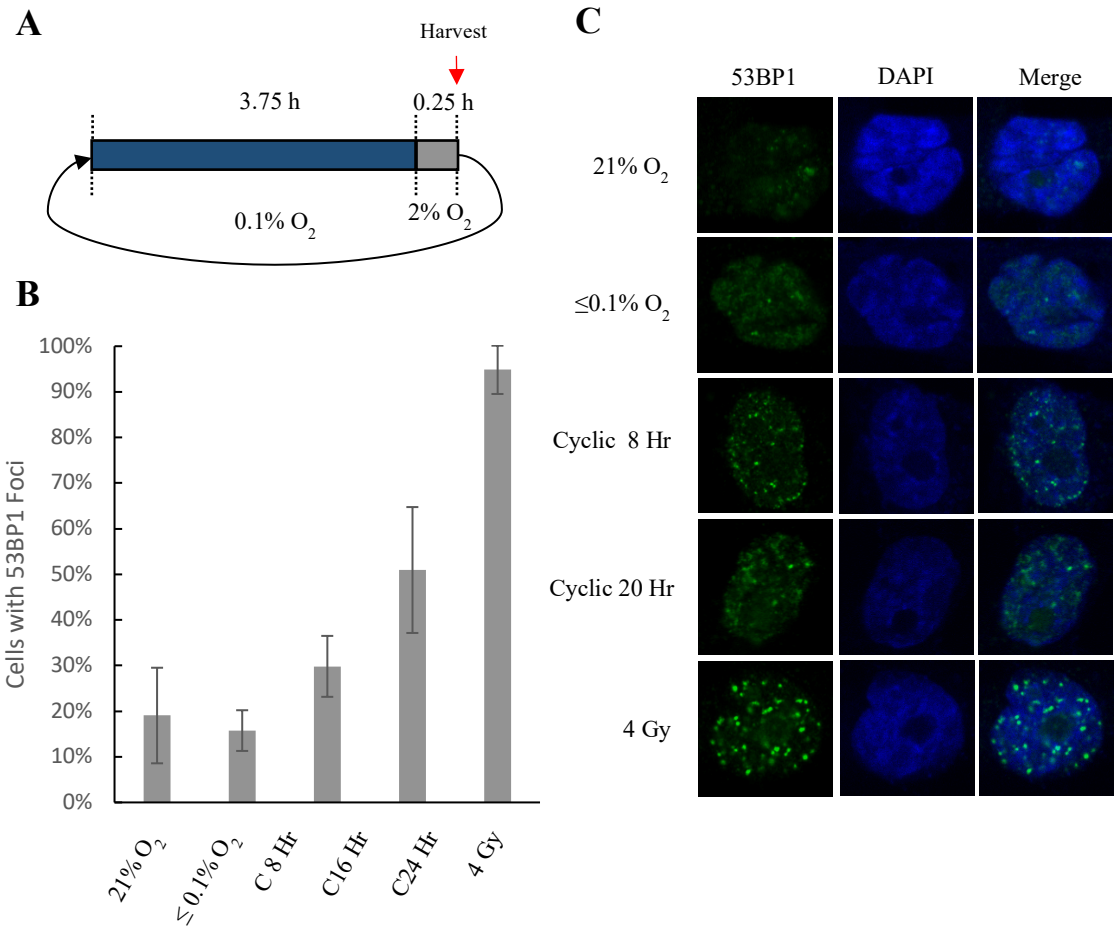

Figure 3.7 A cyclic model of 3.75 hours at ≤0.1% O_2 and 0.25 hours at 2% leads to an accumulation of DNA damage. A) Diagram demonstrating when cells were fixed if harvested in cyclic conditions in contrast to the model used in section 3.3.1. B) Quantification of cells with 53BP1 foci from n=1, error bars represent variation from 10 random image samplings. C) Representative images of cells stained for 53BP1 and DAPI to image the nucleus.

3.4 Regulation of homologous recombination by hypoxia

Exposure to hypoxia, ≤0.1% O_2, has been shown to lead to a decrease in the expression of proteins essential for homologous recombination (HR) (Bindra, et al., 2004). Here, I exposed MDA-MB-231 cells to the three hypoxic conditions and measured the levels of RAD51, an essential HR protein (**Figure 3.8**).

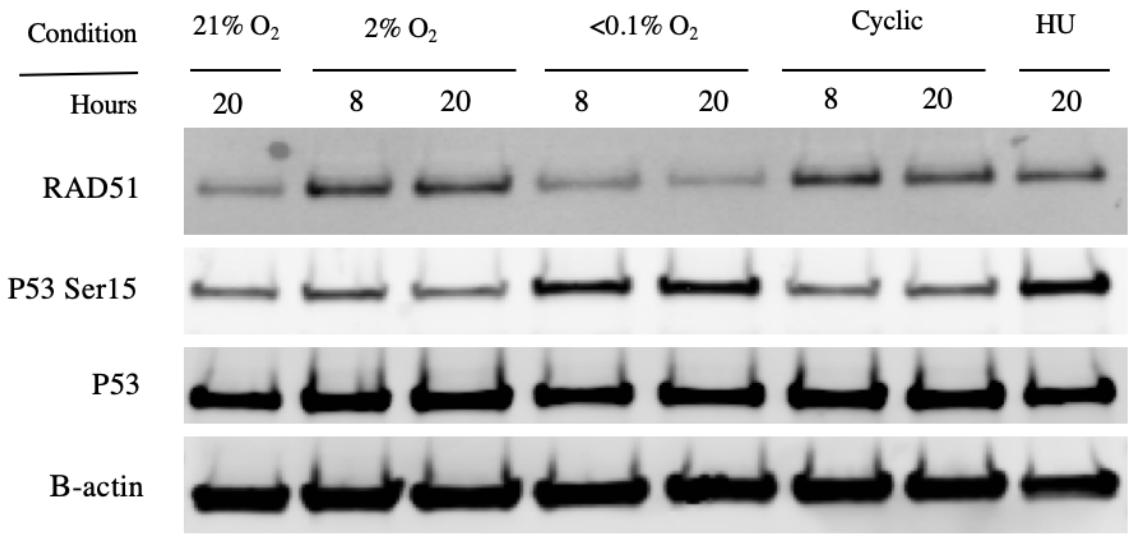

Figure 3.8 Cyclic Hypoxia does not lead to repression of Rad51. MDA-MB-231 Cells were exposed to hypoxic conditions and treated with probed with the antibodies indicated, HU was used at 2mM as a positive control and β-actin was used as a loading control.

As expected, the levels of RAD51 decreased with increasing time in ≤0.1% O_2. In contrast the levels of RAD51 did not decrease in cyclic conditions and appeared to increase, though this may be due to the 2% segment of the cycle as 2% O_2 also shows an increase over normoxic expression. Finding an upregulation of RAD51 in 2% O_2 is very surprising and could not be explained. Further investigation is required.

3.5 Hypoxia-mediated cell viability

Next, I used a colony survival assay to determine the impact of cyclic hypoxic conditions on cell viability. MDA-MB-231 cells were exposed to each hypoxic condition (**Figure 3.9**).

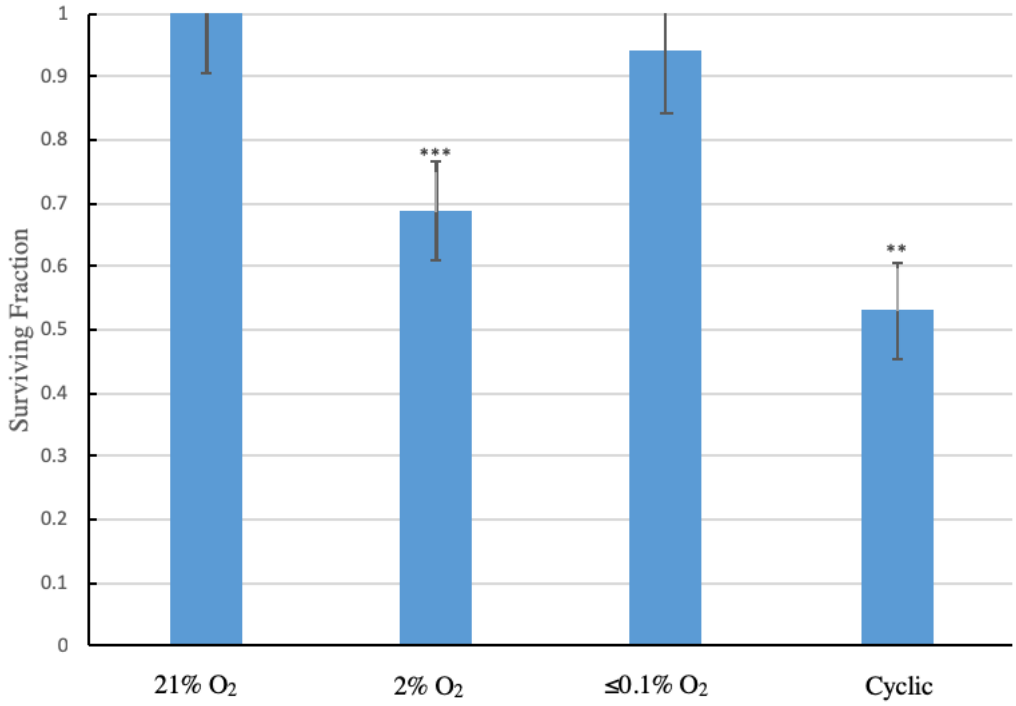

Figure 3.9 Cell viability in hypoxic conditions. MDA-MB-231 cells were exposed to 20 hours of each hypoxic condition as indicated. In the case of cyclic conditions, cells removed from the chamber during the 0% O2 segment of the cycle were removed after 18 hours. Quantification is based off n=3 for 21%, 2%, and ≤0.1% O2 and n=2 for cyclic conditions. Significance: *** $P \leq 0.001$, ** $P \leq 0.01$.

Surprisingly, exposure to 2% O_2 appeared to lead to a greater loss of viability than those in ≤0.1% O_2. This was evident in all three repeats but is not consistent with the literature although these cells may not have been studied previously in these conditions. Interestingly, the cyclic conditions were the most cytotoxic.

3.5.2 Hypoxic Effects on Radiosensitivity

Finally, we attempted to determine the relative radiosensitivity of MDA-MB-231 cells in all three hypoxic conditions. As it is well known that radiosensitivity is determined by oxygen concentration at the exact moment of irradiation, we irradiated cells in cyclic conditions during both the 2 and ≤0.1% O_2 phase of the cycle (**Figure 3.10A**). Irradiating at both phases of the cyclic model allowed me to determine if the biology of cycling acted synergistically with the radiosensitising effect of oxygen concentrations.

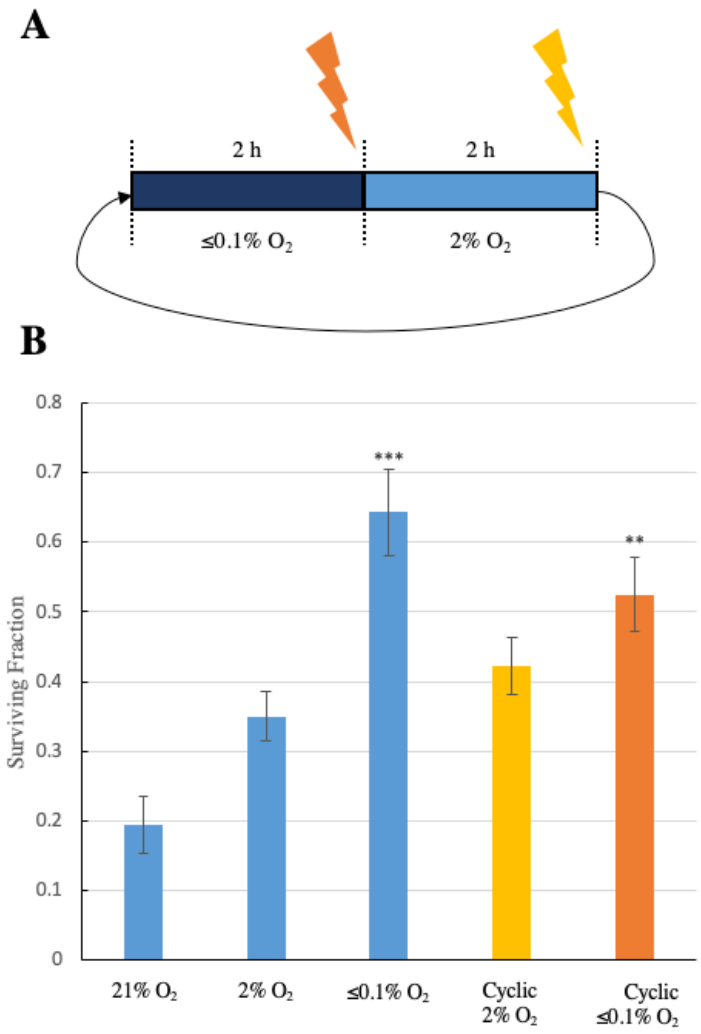

Figure 3.10 Clonogenic survival is determined by oxygen concentration at time of irradiation and not by cyclic conditions. A) Schematic demonstrating two separate irradiated populations, one irradiated at ≤0.1% O_2 (orange) and one at 2% O_2 (yellow). B) Comparison of clonogenic surviving fraction of: 21%, 2%, and ≤0.1%, cyclic ≤0.1%, and cyclic 2% O_2. A t-test comparing each condition to normoxic surviving fraction found ≤0.1% O_2 and cyclic to be significantly more resistant. Significance: *** P ≤ 0.001, ** P ≤ 0.01. n=2

The cells exposed to ≤0.1% O_2 were the most radiation resistant with 3.3 times as many cells achieving clonogenic survival. Exposure to 2% O_2 also increased radiation sensitivity although less significantly. Interestingly, the cells in cyclic hypoxia, harvested at both 2 and ≤0.1% O_2, were more radiation resistant than those at 2% O_2 but less resistant than those at ≤0.1% O_2. As expected the cyclic cells irradiated whilst at ≤0.1% O_2 were more resistant than those irradiated at 2% O_2 (**Figure 3.10B**).

Cyclic resistance at 2% O_2 is an interesting result in light of finding a reduced viability as a result of cyclic conditions (**figure 3.9**). Predisposed cell death did not seem to have an impact on radiosensitivity. It is also interesting that Constant ≤0.1% O_2 remains more resistant than cyclic ≤0.1% O_2, despite a known reduction in DNA repair machinery. This suggests that viability was determined by DNA damage (least of which would be in ≤0.1% O_2) and not by reduction in RAD51.

4. DISCUSSION

Here, I have described the biological response to three different hypoxic conditions all of which are physiologically relevant (2, ≤0.1% O_2 and cycling between the two). I found that cycling between these two oxygen concentrations gives rise to a significant S phase accumulation while maintaining a normal mitotic index. While cumulative damage was found after reducing the length of the 2% O_2 segment, no damage was found when two hours was allowed for reoxygenation. Both cyclic segments (2% and ≤0.1% O_2) are more resistant than MDA-MB-231 cells radiated at 2%, though neither were as resistant as constant ≤0.1% O_2.

Finding these differences in cell cycle distribution, cell viability, and radioresistance highlights a shortfall in the hypoxia literature. Studying hypoxia at constant levels—while a good baseline—may be a model that needs to be left behind. Recreating a more accurate environment can both highlight new therapeutic targets and alert us to efficacy of current targets. This project has highlighted that there are significant differences between standard laboratory models and those found in physiological studies.

A limitation of this study is that we have primarily focused on one set of cycling conditions. Although cyclic hypoxia is a well-described phenomenon, the specific timings and amplitude of fluctuations have rarely been measured. The cyclic schedule used here was determined based on the work of Professor Mark Dewhirst (2009). Another factor in choosing this model was the equipment used. The Don Whitley Chamber used in this project—due to total volume—is limited in how quickly it can cycle. Were there more time for this project, other pieces of equipment such as the OxyGenie™ [Baker] could have been used to explore a more rapid cycling model. Alternative cycling conditions could have a large impact on radiosensitivity especially given that the schedule shown in Figure 3.7 showed an accumulation of DNA damage. This would could predict an increase radiosensitivity. Unfortunately, these altered cyclic conditions were only used towards the end of the research project.

While no DNA damage was found at the end of the cyclic 2% O_2 segment, it was shown that reoxygenation from 0% O_2 to 2% O_2 does cause damage (Figure 3.7). A likely explanation for this is that 2 hours is sufficient time to repair this damage. Altering the cycling conditions to a shorter model

(<1 Hour) could prevent this repair and enhance radiodensity. It would be equally interesting to determine whether a rapid cycle would also alter cell cycle distribution as was seen in this project.

In contrast to the data shown here, Kumareswaran et al. found no change in RAD51 expression in cyclic hypoxia compared to normoxic conditions (2015). Kumareswaran et al. used two cycles, one cycling between 30 minutes of 0% O_2 followed by 30 minutes at 7% O_2 and the other being 3 hours at 0% O_2 and 7% O_2 for 30 minutes. In both these models they found no difference in expression of RAD51. It is possible that this is a cell line dependent finding (Kumareswaran et al. used H1299 human lung carcinoma cells). Testing these findings in several more cell lines—both cancerous and normal—would be very helpful in identifying the reason for these findings. It is not understood why RAD51 appears to be upregulated in 2% O_2 in this project. Work done by Calvo-Asensio et al. would suggest that there should be no change in RAD51 expression as a result of prolonged exposure to 2% O_2 (2018). It may be that higher oxygen concentrations (such as 7% used by Kumareswaran et al.) do not induce this.

Another key limitation to this project is its focus on cyclic hypoxia prior to irradiation but not following. Colonies were returned to normoxic conditions after irradiation. Noting upregulation in RAD51 and S phase accumulation, returning cells back to cyclic conditions post irradiation may enhance resistance due to greater use of HR. While this study has shown connections to two of the five R's of fractionation (repair and redistribution), understanding the full implications of this requires studying the effects of cyclic hypoxia post irradiation.

This project has shown that there are significant biological changes as a result of cyclic hypoxia, demonstrating that this is a feature of the microenvironment worth studying. The next step in this work should be to identify the effects that cycle length and oxygen concentration has on these changes. Better understanding the consequences of the tumour microenvironment can only improve clinical outcomes.

5. Acknowledgments

I want to thank my PI, Ester Hammond, for helping me so greatly in my short time at Oxford. She has guided my project and offered invaluable support in writing this thesis. She also introduced me to cricket.

Samuel Bader taught me and remained patient with my simple questions throughout this project. His curiosity for science and interest in cyclic hypoxia has acted as an inspiration for myself. I hope we are able to work together in the future.

Joseph Wilson has been a lab mate, fellow student of medicine, and friend. He helped me enormously in both lab and in life. Without him, my time in Oxford would not have been as bright.

Finally, I want to acknowledge my course mates Collin, Anouk, Y.C., Ayesha, and Janine—with whom I've made lifelong friends.

6. APPENDIX

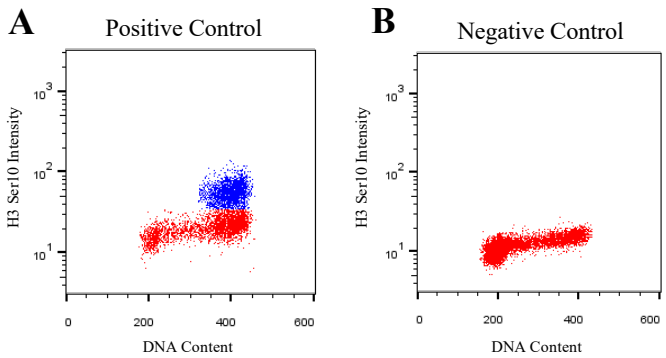

Figure 6.1 Positive and negative controls for H3 Ser10 FACS analysis (section 3.1.3). **A)** In the positive control, cells were subjected to microtubule poison Colcemid (0.1 µg/ml KaryoMAX® Gibco). This acts as a mitotic trap, resulting in 49.1% of cells stuck in mitosis and therefore being H3 Ser10 positive while 4N. **B)** The negative control was prepared in the same conditions described in section 2.7.2 with the exception of not receiving a secondary antibody. No cells were found to be H3 Ser10 positive, excluding the possibility of autofluorescence.

7. REFERENCES

Baudelet, C. et al., 2004. Physiological noise in murine solid tumours using T2∗-weighted gradient-echo imaging: a marker of tumour acute hypoxia?. *Physics in Medicine and Biology,* Issue 49, pp. 3389-3411.

Bencokova, Z. et al., 2009. ATM Activation and Signaling under Hypoxic Conditions. *Molcular and Cellular Biology,* 29(2), pp. 526-537.

Bennewith, K. L. & Durand, R. E., 2004. Quantifying Transient Hypoxia in Human Tumor Xenografts by Flow Cytometry. *Cancer Research,* 64(17), pp. 6183-6189.

Bindra, R. et al., 2004. Down-Regulation of Rad51 and Decreased Homologous Recombination in Hypoxic Cancer Cells. *Molecular and Cellular Biology,* 24(19), pp. 8504-8518.

Brahimi-Horn, C. M., Chiche, J. & Pouysségur, J., 2007. Hypoxia and cancer. *Journal of Molecular Medicine,* Issue 85, pp. 1301-1307.

Bristow, R. & Hill, R. P., 2008. Hypoxia, DNA repair and genetic instability. *Nature Review Cancer,* Volume 8, pp. 180-192.

Brown, G., Hafner, R. & Brand, M., 1990. A 'top-down' approach to the determination of control coefficients in metabolic control theory.. *European Journal of Biochemistry,* Issue 188, pp. 321-325.

Brown, J. M. & Wilson, W. R., 2004. Exploiting Tumour Hypoxia in Cancer Treatment. Volume 4.

Cairns, R. & Hill, R., 2004. Acute hypoxia enhances spontaneous lymph node metastasis in an orthotopic murine model of human cervical carcinoma. *Cancer Research,* Issue 64, pp. 2054-2061.

Calvo-Asensio, I., Dilon, E. T., Lowndes, N. F. & Ceredig, R., 2018. The Transcription Factor Hif-1 Enhances the Radio-Resistance of Mouse MSCs. *Fronteirs in Physiology,* 9(439), pp. 1-18.

Carpenter, T. et al., 2003. Hypoxia reversibly inhibits epithelial sodium transport but does not inhibit lung ENaC or Na-K-ATPase expression. *About American Journal of Physiology-Lung Cellular and Molecular Physiology,* Issue 284, pp. L77-L83.

Chandel, N., Budinger, G., Choe, S. & Schumacker, P., 1997. Cellular respiration during hypoxia. Role of cytochrome oxidase as the oxygen sensor in hepatocytes. *Journal of Biological Chemistry,* Issue 272, pp. 18808-18816.

Chang, Q., Jurisica, I., Do, T. & Hedley, D. W., 2011. Hypoxia Predicts Aggressive Growth and Spontaneous Metastasis Formation from Orthotopically Grown Primary Xenografts of Human Pancreatic Cancer. *Cancer Research,* 71(8), pp. 3110-3120.

Chaplin, D., Durand, R. & Olive, P., 1986. Acute Hypoxia in Tumours: Implicaitons for Modiifiers of Radiation Effects. *International Journal of Radiation Oncology, Biology, Physics,* Volume 12, pp. 1279-1282.

Chaundary, M. & Hill, R., 2009. Increased expression of metastasis- related genes in hypoxic cells sorted from cervical and lymph nodal xenograft tumors. *Laboratory Investigation,* Issue 89, pp. 587-596.

Clementi, E., Brown, G., Foxwell, N. & S, M., 1999. *On the mechanism by which vascular endothelial cells regulate their oxygen consumption.* s.l., Proceedings of the National Academy of Sciences of the United States of America.

Denekamp, J., 1999. Inducible repair and the two forms of tumour hypoxia–time for a paradigm shift.. *Acta Oncologica,* 38(7), pp. 903-918.

Dewhirst, M. W., 2009. Relationships between Cycling Hypoxia, HIF-1, Angiogenesis and Oxidative Stress. *Radiation Research,* Issue 172, pp. 653-665.

Dings, J., Meixensberger, J., Jager, A. & Roosen, K., 1998. Clinical experience with 118 brain tissue oxygen partial pressure catheter probes. *Neurosurgery,* Issue 43, pp. 1082-1095.

Evans, S. M. et al., 2004. Hypoxia Is Important in the Biology and Aggression of Human Glial Brain Tumors. *Clinical Cancer Resesarch,* 10(24), pp. 8177-8184.

Graeber, T. G. et al., 1996. Hypoxia-mediated selection of cells with diminished apoptotic potential in solid tumours. *Nature,* Issue 379, pp. 88-91.

Gray, L. e. a., 1953. The concentration of oxygen dissolved in tissues at the time of irradiation as a factor in radiotherapy. *British Journal of Radiology,* Issue 26, p. 638.

Grimes, D. & Partridge, M., 2015. A mechanistic investigation of the oxygen fixation hypothesis and oxygen enhancement ratio. *Biomedical Physics & Engineering Express,* 1(4).

Höckel, M. et al., 1992. Intratumoral pO2 predicts survival in advanced cancer of the uterine cervix. *Radiotherapy and Oncology,* Issue 26, pp. 45-50.

Hall, E. J. & Giaccia, A. J., 2019. *Radiobiology for the Radiobiologist.* 8th Edition ed. Philidelphia: Wolters Kluwer.

Hammond, E. et al., 2014. The meaning, measurement and modification of hypoxia in the laboratory and the clinic. *Clinical Oncology (The Royal College of Radiologists),* Volume 26, pp. 277-288.

Hammond, E., Dorie, M. & Giaccia, M., 2003. ATR/ATM targets are phosphorylated by ATR in response to hypoxia and ATM in response to reoxygenation. *The Journal of Biological Chemistry,* 14(278), pp. 12207-12213.

Hammond, E., Dorie, M. J. & Giaccia, A., 2004. Inhibition of ATR Leads to Increased Sensitivity to Hypoxia/Reoxygenation. *Cell and Tumour Biology,* 64(18), pp. 6556-6562.

Hanahan, D. & Weinberg, R., 2011. Hallmarks of Cancer: the Next Generation. *Cell,* Issue 144, pp. 646-674.

Ho, F., Tsang, W., Hong, S. & Kwok, T., 2006. The critical role of caspases activation in hypoxia/reoxygenation induced apoptosis.. *Biochemical and Biophysical Research Communications,* 345(3), pp. 1131-1137.

Horsman, M. R. et al., 2012. Imaging hypoxia to improve radiotherapy outcome. *Nature Reviews Clinial Oncology,* 9(12), pp. 674-687.

Hu, C. et al., 2003. Differential roles of hypoxia-inducible factor 1 alpha (HIF1alpha) and HIF-2alpha in hypoxic gene regulation. *Molecular Cellular Biology,* 23(24), pp. 9361-9374.

Keith, B., Johnson, R. & Simon, M., 2011. HIF1alpha and HIF2alpha: sibling rivalry in hypoxic tumour growth and progression. *Nature Review Cancer,* 12(1), pp. 9-22.

Kim, J., Tchernyshyov, I., Semenza, G. & Dang, C., 2006. HIF-1-mediated expression of pyruvate dehydrogenase kinase: a metabolic switch re- quired for cellular adaptation to hypoxia. *Cellualar Metabolism,* Volume 3, pp. 177-185.

Kimura, H. et al., 1996. Fluctuations in Red Cell Flux in Tumor Microvessels Can Lead to Transient Hypoxia and Reoxygenation in Tumor Parenchyma. *Cancer Research,* Issue 56, pp. 5522-5528.

Koh, M. & Powis, G., 2012. Passing the baton: the HIF switch. *Trends in Biochem Science,* Volume 37, pp. 364-372.

Kumareswaran, R. et al., 2015. Cyclic hypoxia does not alter RAD51 expression or PARP inhibitor cell kill in tumor cells Ramya. *Radiotherapy and Oncology,* Issue 116, pp. 388-391.

Lanzen, J. et al., 2006. Direct Demonstration of Instabilities in Oxygen Concentrations within the Extravascular Compartment of an Experimental Tumor. *Cancer Research,* 66(4), pp. 2219-2223.

Lee, V. et al., 2002. Hypoxia sensitizes cells to nitric oxide-induced apoptosis. *Journal of Biological Chemistry,* Issue 277, pp. 16067-16074.

Le, Q. et al., 2006. An evaluation of tumor oxygenation and gene expression in patients with early stage non-small cell lung cancers. *Clinical Cancer Research,* Volume 12, pp. 1507-1514.

Lukas, C. et al., 2011. 53BP1 Nuclear Bodies Form Around DNA Lesions Generated by Mitotic Transmission of Chromosomes Under Replication Stress. *Nature Cell Biology,* Issue 13, pp. 243-253.

Mimitou EP, S. L., 2011. DNA Resection-Unraveling the Tail. *DNA Repair,* Issue 10, pp. 344-348.

Mole, D. et al., 2009. Genome-wide Association of Hypoxia-Inducible Factor (HIF)-1alpha and HIF-2alpha DNA Binding With Expression Profiling of Hypoxia-Inducible Transcripts. *Journal ofBiological Chemistry,* 25(284), pp. 16767-16775.

Olcina, M. M., Grand, R. J. & Hammond, E. M., 2014. ATM activation in hypoxia - causes and consequences. *Molecular Cellular Oncology,* 1(1), p. e29903.

Pacek M, W. J., 2004. A Requirement for MCM7 and Cdc45 in Chromosome Unwinding During Eukaryotic DNA Replication. *European Molecular Biology Organization,* Issue 23, pp. 3667-3676.

R. H. Thomlinson, L. H. G., 1955. The Histological Structure of Some Human Lung Cancers and the Possible Implications for Radiotherapy. *British Journal of Cancer,* 9(4), pp. 539-549.

Rofstad, E. K. et al., 2010. Tumors exposed to acute cyclic hypoxic stress show enhancedangiogenesis, perfusion and metastatic dissemination. *International Journal of Cancer,* Issue 127, pp. 1535-1546.

Saikumar, P., Dong, Z., Weinberg, J. M. & MA, V., 1998. Mechanisms of Cell Death in Hypoxia/Reoygenation Injury. *Oncogene,* Issue 17, pp. 3341-3349.

Serocki, M. et al., 2018. miRNAsregualte te HIF Switch During Hypoxia: a Novel Therapeutic Target. *Angiogenesis,* Issue 21, pp. 183-202.

Skala, M. C. et al., 2009. Combined hyperspectral and spectral domain optical coherence tomography microscope for noninvasive hemodynamic imaging. *Optics Letters,* 34(3), pp. 289-291.

Vaupel, P., 2004. Tumor microenvironmental physiology and its implications for radiation oncology. *Seminars in Radiation Oncology,* 14(3), pp. 198-206.

Vaupel, V. & Mayer, A., 2007. Hypoxia in cancer: significance and impact on clinical outcome. *Cancer and Metastisis Reviews,* 26(2), pp. 225-239.

Virchow, R., 1863. *Die Krankhaften Geschwülste.* Berlin: Hirschwald.

Wang, W., Winlove, C. & Michel, C., 2003. Oxygen partial pressure in outer layers of skin of human finger nail folds. *Journal of Physiology,* Volume 549, pp. 855-863.

Wigerup, C., Påhlman, S. & Bexell, D., 2016. Therapeutic targeting of hypoxia and hypoxia-inducible factors in cancer. *Pharmacology and Therapeutics,* Issue 164, pp. 152-169.

Yasui, H. et al., 2010. Low-Field Magnetic Resonance Imaging to Visualize Chronic and Cycling Hypoxia in Tumor-Bearing Mice. *Cancer Research,* 70(16), pp. 6427-6436.